CREB1 acts via the miR-922/*ARID2* axis to enhance malignant behavior of liver cancer cells

XINYU LIU[1], HAO ZHANG[2], PENGCHENG ZHOU[1,3], YAQUN YU[4], HAOYE ZHANG[1], LIMIN CHEN[1], JIAN GONG[1] and ZHENGUO LIU[1,3]

Departments of [1]Infectious Disease and [2]Nephrology, The Third Xiangya Hospital, Central South University, Changsha, Hunan 410013; [3]Hunan Key Laboratory of Viral Hepatitis, Xiangya Hospital, Central South University, Changsha, Hunan 410008; [4]Department of Hepatobiliary and Pancreatic Surgery, The Affiliated Hospital of Guilin Medical College, Guilin, Guangxi 541002, P.R. China

Received August 13, 2020; Accepted February 18, 2021

DOI: 10.3892/or.2021.8030

Abstract. There is little information on the role of microRNA (miR)-922 in the malignant behavior of liver cancer. The present study investigated the regulation of miR-922 expression levels by cAMP response element binding protein 1 (*CREB1*) in liver cancer tissue, its role in regulating malignant behavior and its potential targets in liver cancer. miR-922 expression in liver cancer cells and tissue was determined by reverse transcription-quantitative PCR. The binding of *CREB1* to the promoter region of mir-922 was tested by chromatin immunoprecipitation-PCR. The predicted AT-rich interactive domain 2 (*ARID2*) and fidgetin, microtubule severing factor targets of miR-922 were characterized by dual luciferase reporter assay. The effects of altered *ARID2* expression levels on miR-922-enhanced malignant behavior of liver cancer cells were tested. *CREB1* bound to the promoter region of miR-922. Elevated miR-922 transcripts were inversely associated with *ARID2* expression in liver cancer tissue and cells. miR-922 inhibited *ARID2*-regulated luciferase expression and was present in the miR/argonaute RISC catalytic component 2 complex. *ARID2* significantly decreased malignant behavior of liver cancer MHCC97L cells. Similarly, *ARID2* over-expression inhibited growth of xenograft liver cancer tumors and decreased miR-922, Bcl-2, proliferating cell nuclear antigen, cyclin D1, *MMP3* and *MMP9* expression and serum VEGF and TNF-α levels, but enhanced Bax expression levels in tumors. *ARID2* over-expression abrogated malignant behavior promoted by miR-922 over-expression and enhanced miR-922-decreased malignant behavior of liver cancer cells. *CREB* induced miR-922 transcription, which targeted *ARID2* to enhance malignant behavior of liver cancer cells, indicating that the *CREB1*/miR-922/*ARID2* axis may be a potential target for liver cancer treatment.

Correspondence to: Dr Zhenguo Liu, Department of Infectious Disease, The Third Xiangya Hospital, Central South University, 138 Tongzipo Road, Changsha, Hunan 410013, P.R. China
E-mail: liuzg729@163.com

Abbreviations: ARID2, AT-rich interactive domain 2; *CREB1*, cAMP response element binding protein 1; HCC, hepatocellular carcinoma; miRNA, microRNA

Key words: liver cancer, miRNA, *CREB1*, *ARID2*, proliferation, metastasis

Introduction

Liver cancer is a common type of neoplasia and has the second highest rate of cancer-associated mortality in the world (1). More than 90% of primary liver cancer cases are hepatocellular carcinoma (HCC). In China, the 5-year survival of HCC is only 12.1% (2). Etiologically, hepatitis B and C virus infection-associated fibrosis and cirrhosis are the most common risk factors for the development of liver cancer (3). Although therapeutic approaches, such as surgical resection, chemotherapy and immunotherapy, have advanced, liver cancer remains a major threat (4) because many patients with liver cancer are diagnosed at advanced stage and prone to development of multi-drug resistance. Hence, novel therapeutic targets for intervention and more reliable biomarkers for early diagnosis of liver cancer are urgently needed (4).

MicroRNAs (miRNAs or miRs), ~23 nucleotides in length, are key members of the non-coding RNA family (5). miRNAs control expression of their target mRNAs principally by binding to the 3'-untranslated region (3'-UTR) to inhibit the translation of mRNA and decrease its half-life. miR-922 is a tumor-promoting gene that promotes the development and progression of tumors (6,7). miR-922 expression levels are decreased in breast cancer (8). By contrast, miR-922 expression is significantly upregulated in hepatocellular carcinoma (HCC) tissue and promotes proliferation of HCC cells by targeting cylindromatosis (CYLD) to enhance c-Myc and cyclin D1 expression levels and inhibit retinoblastoma (Rb) phosphorylation (8). However, the role of miR-922 in regulating the malignant behavior of liver cancer cells is still unclear.

cAMP response element binding protein 1 (*CREB1*) is a member of the leucine zipper transcription factor family and enhances HCC progression by promoting angiogenesis

and resistance to apoptosis (9). Upregulated *CREB1* expression levels and phosphorylation have been detected in HCC tissue (10). Furthermore, *CREB1* also mediates hepatitis B virus X protein-cortactin interactions to promote malignant behavior of HCC cells (11). AT-rich interactive domain 2 (*ARID2*) is a tumor suppressor and member of the switch/sucrose non-fermentable chromatin remodeling complex (12). *ARID2* knockout disrupts DNA damage responses by inhibiting recruitment of xeroderma pigmentosum complementation group G (12). To the best of our knowledge, however, there is no information on whether miR-922 targets and regulates *ARID2* expression and its effect on malignant behavior of liver cancer cells.

The present study validated miR-922 expression levels in 10 pairs of liver cancer and adjacent tissue, liver cancer cells and non-tumor hepatocytes. The aim was to determine how *CREB1* regulates miR-922 expression levels in liver cancer cells. The impact of *ARID2*, a potential target of miR-922, on the malignant behaviors of liver cancer cells was also investigated both *in vitro* and *in vivo*.

Materials and methods

Clinical samples. The present study was approved by the Ethics Committee of the Third Xiangya Hospital of Central South University and all patients provided written informed consent. Liver cancer and matched adjacent (distance, >3 cm) non-tumor hepatic tissue (10 pairs) were collected from patients with liver cancer during surgical treatment between September 2018 and September 2019 in The Third Xiangya Hospital of Central South University, China (Table I). All samples were collected with signed informed consent. Patients were diagnosed based on the practice guidelines of the American Association for the Study of Liver Diseases (13). Liver specimens were evaluated by pathologists and clinical stage was determined according to the Barcelona Clinic Liver Cancer classification (14). Exclusion criteria were as follows: i) patients ≤18 or ≥70 years of age or without full civil capacity to provide informed consent; ii) history of preoperative anticancer radiotherapy or chemotherapy, biological, immune or traditional Chinese medicine therapy; iii) incomplete postoperative follow-up data and iv) history of another organ malignancy or systemic immune disease.

Cell culture and transfection. Human liver cancer HepG2, MHCC97H, MHCC97L and non-tumor hepatic THLE-2 cells were purchased from the Cell Bank of China (Shanghai, China). THLE-2 cells were cultured in RPMI-1640; other cells were cultured in DMEM supplemented with 10% fetal bovine serum (all Thermo Fisher Scientific, Inc.) at 37˚C in 5% CO_2. The authenticity of all cell lines was tested by STR (Shanghai Yihe Applied Biotechnology Co., Ltd. and Guangzhou Cellcook Biotech Co., Ltd.).

HepG2 and MHCC97L cells were transfected with control plasmid (pcDNA3.1-NC) or plasmid for the expression of *ARID2* [pcDNA3.1-ARID2 (OE), GeneCopoeia, Inc.] using Lipofectamine® 3000 (Thermo Fisher Scientific, Inc.) and treated with 1 mg/ml G418 for 3 weeks to generate control HepG2/MHCC97L-overexpression (OE)-negative control (NC) or ARID stable expressing HepG2/MHCC97L-*ARID2*-OE cells. HepG2/MHCC97L, HepG2/MHCC97L-NC and HepG2/MHCC97L-*ARID2*-OE cells were transfected with control scramble miRNA, miR-922 mimics or miR-922 inhibitor (Guangzhou RiboBio Co., Ltd.) for 48 h at 37˚C. In addition, HepG2/MHCC97L cells were transduced with control lentivirus or lentivirus for expression of ARID-specific short hairpin (sh)RNA [pGPU6/GFP-ARID2 (sh)] in the presence of 4 μg/ml puromycin for 4 days to generate control HepG2/MHCC97LshRNA-NC and ARID stably silencing HepG2/MHCC97L-*ARID2*sh cells. Subsequent experiments were performed 48 h after transfection.

Reverse transcription-quantitative (RT-q)PCR. Total RNA was extracted from individual groups of cells (THLE-2, HepG2, MHCC97H and MHCC97L) using TRIzol® reagent and reverse transcribed into cDNA using a PrimeScript RT reagent kit (Invitrogen; Thermo Fisher Scientific, Inc.) according to the manufacturer's protocol. The relative levels of miRNA and mRNA transcripts to control U6 and GAPDH were quantified by RT-qPCR in duplicate using SYBR Premix Ex Taq (Takara Biotechnology Co., Ltd.) and specific primers (Table II). Thermocycling conditions were as follows: Initial denaturation at 94˚C for 10 min, followed by 40 cycles of 94˚C for 30 sec, 60˚C for 30 sec and 72˚C for 10 sec and final extension at 72˚C for 8 min. The data were analyzed by $2^{-\Delta\Delta Cq}$ method (15).

Cell proliferation assay. The HepG2 and MHCC97L cell proliferation was determined by Cell Counting Kit-8 (CCK-8) assay (Dojindo Molecular Technologies, Inc.) according to the manufacturer's protocol. The absorbance at 450 nm was measured using a microplate reader following incubation for 1-2 h.

Wound healing assay. After serum-starved HepG2 and MHCC97L cells in each group reached 100% confluence, they were wounded with a plastic tip. The cells were cultured for 24 h at 37˚C. Wound width was measured at 0 and 24 h under a light microscope (magnification, x100).

Transwell invasion assay. The HepG2 and MHCC97L cells ($1x10^5$ cells/well) were starved overnight, then cultured in the upper chamber pre-coated (37˚C for 30 min) with Matrigel (BD Biosciences) of 24-well Transwell plates (pore size, 8 μm; Corning, Inc.). The bottom chamber was filled with complete medium supplemented with 10% FBS (Thermo Fisher Scientific, Inc.). The cells were cultured for 48 h at 37˚C, fixed with 10% glutaraldehyde at 4˚C for 30 min and stained with 1% crystal violet for 20 min at room temperature, followed by photoimaging under a light microscope (Olympus Corporation) at 100x magnification.

Colony formation assay. Each group of cells (300 cells/well) was cultured in 6-well plates for 2 weeks at 37˚C. The formed cell colonies were fixed with 4% formaldehyde for 15 min at room temperature and stained with 1% crystal violet for 20 min at room temperature, followed by counting in a blinded manner.

Chromatin immunoprecipitation (ChIP). Potential binding of *CREB1* to the promoter region of miR-299 was determined by ChIP assay as previously described (16). Briefly,

Table I. Expression levels of mir-922 and *ARID2* in patients with hepatocellular carcinoma.

Characteristic		n	miR-922		*ARID2*	
			Mean ± SD	P-value	Mean ± SD	P-value
Sex	Male	7	9.366±3.475	0.842	0.301±0.163	0.315
	Female	3	8.986±2.209		0.194±0.048	
Age, years	≤50	4	7.806±2.489	0.238	0.374±0.173	0.053
	>50	6	10.216±3.162		0.199±0.070	
AFP, ng/ml	<20	2	6.803±0.139	0.027	0.479±0.107	0.010
	≥20	8	9.864±3.105		0.216±0.097	
HBsAg	Positive	10	9.252±3.028		9.252±3.028	
	Negative	0				
Cirrhosis	Positive	8	9.924±3.024	0.020	0.299±0.146	0.195
	Negative	2	6.562±0.633		0.146±0.021	
Tumor size, cm	≤5	7	8.312±2.263	0.141	0.314±0.149	0.130
	>5	3	11.446±3.947		0.161±0.046	
Tumor number	1	8	8.686±3.155	0.039	0.298±0.147	0.210
	≥2	2	11.517±0.167		0.149±0.163	
Tumor stage	I/II	6	7.687±1.956	0.035	0.340±0.146	0.047
	III/IV	4	11.599±2.980		0.161±0.381	
Distant metastasis	No	8	8.303±2.444	0.037	0.321±0.131	0.116
	Yes	2	13.050±2.150		0.150±0.016	

miR, microRNA; *ARID2*, AT-rich interactive domain 2; AFP, α fetoprotein; HBsAg, hepatitis B surface antigen.

MHCC97L and HepG2 cells were transfected with scramble control or *CREB1*-specific shRNA (Table II) for 48 h and the efficacy of *CREB1* silencing was verified by western blotting as aforementioned. The control and *CREB1*-silenced cells were cross-linked with 1% formaldehyde for 10 min at room temperature and sonicated on ice to generate ~500-bp DNA fragments. Following centrifugation (14,000 x g; 10 min; 4˚C), the obtained soluble chromatin samples were reacted with anti-CREB 1 (1:10; cat. no. ab31387; Abcam), anti-H3K27me3 (1:10; cat. no. ab6002; Abcam), anti-H3K27AC (1:10; cat. no. ab4729; Abcam) or control IgG (1:10; cat. no. ab171870; Abcam) overnight at 4˚C. The immunocomplex was precipitated by Protein A Agarose/Salmon Sperm DNA (50% Slurry) beads and eluted. DNA fragments were analyzed by qPCR, as aforementioned, using specific primers (Table II).

Luciferase reporter gene assay. Hsa-miR-922 mimics and hsa-miR-922 inhibitor were designed and synthesized by Shanghai GenePharma Co., Ltd. as follows: Mimics forward, 5'-GCAGCAGAGAAUAGGACUACGUC-3' and reverse, 5'-CGUAGUCCUAUUCUCUGCUGCUU-3'; inhibitor 5'-GACGUAGUCCUAUUCUCUGCUGC-3' and NC forward, 5'-UUCUCCGAACGUGUCACGUTT-3' and reverse, 5'-ACGUGACACGUUCGGAGAATT-3'. Reporter plasmid pmirGLO Dual-Luciferase miRNA Target Expression Vector was obtained from Promega Corporation. Transfection was performed using Lipofectamine® 2000 (cat. no. 11668030; Thermo Fisher Scientific, Inc.) and Dual-Glo® Luciferase Assay system (cat. no. E2920; Promega Corporation) was used for luciferase assay. DNA fragments for the 3'UTR of fidgetin, microtubule severing factor (*FIGN*) and *ARID2* were cloned and the specific motifs for miR-922 binding were mutated using QuikChange Site-Directed Mutagenesis kit (Stratagene; Agilent Technologies, Inc.), according to the manufacturer's instructions. The wild-type (WT) and mutant (MT) 3'UTR of *FIGN* and *ARID2* were cloned into the 3'-end of firefly luciferase of the Dual-luciferase Target Vector (Promega Corporation). Subsequently, MHCC97L cells were co-transfected with miR-922 mimic, together with the plasmid for WT or MT FIGN and *ARID2* reporter and plasmid for *Renilla* luciferase expression for 48 h. After 48 h, the medium in the 96-well plate was discarded before washing twice with PBS. A total of 100 μl diluted 1X Dual-Glo Luciferase Assay Reagent was added to each well before shaking at 25˚C for 15 min. Luminescence activity was detected and normalized to that of *Renilla* luciferase.

In addition, the miR-922 promoter region (2,000 bp upstream of transcription initiation site) was cloned into the Dual-luciferase Target Vector to control firefly luciferase expression. Then, 293T cells were co-transfected with plasmids for the firefly luciferase reporter, *CREB1* and *Renilla* luciferase expression. The regulatory effect of *CREB1* on the miR-922 promoter-controlled luciferase expression was determined by Dual-Luciferase Reporter Assay system. The control cells received plasmids for firefly luciferase reporter and *Renilla* luciferase expression, as well as an empty plasmid without enhanced *CREB1* expression.

In situ hybridization. Digoxigenin (Dig)-labelled probe (5'-GCAGCAGAGAAUAGGACUACGUC-3') for miR-922 was designed and synthesized by BersinBi. The distribution of

Table II. Primer sequences.

Gene		Sequence (5'→3')
GAPDH	Forward	caatgacccttcattgacc
	Reverse	gacaagcttcccgttctcag
β catenin	Forward	atgactcgagctcagagggt
	Reverse	attgcacgtgtggcaagttc
microRNA-922	Forward	gcagcagagaataggactacgtc
	Reverse	tggtgtcgtggagtcg
CREB1 promoter region		
0-200 bp from TSS	Forward	agtaagagggccagggttca
	Reverse	atgtcccaggtttcctccct
200-400 bp from TSS	Forward	ggactgaaaatgatccgctgc
	Reverse	ctgcagctgtctcttacccc
400-600 bp from TSS	Forward	gccggtagagaaggaaaggt
	Reverse	gttgtccttcctggtactcca
800-1,000 bp from TSS	Forward	cggagtccagaatcgaaccc
	Reverse	ctcggcctcctaaagtggtg
1,000-1,200 bp from TSS	Forward	tactagggaggctgaggcag
	Reverse	gagtctagcccttgtcgcc
1,200-1,400 bp from TSS	Forward	gagagggctgcagagttcac
	Reverse	tctacagcagggattcgcac
1,400-1,600 bp from TSS	Forward	catatttccaggggtccggg
	Reverse	cccgatactgtggcaccttg
1,600-1,800 bp from TSS	Forward	cagcagaccttcttccccag
	Reverse	cctggctctgctcttgacc
1,800-2,000 bp from TSS	Forward	tttccaccaagtcgccgac
	Reverse	cggctttcgcatcggtaaag

CREB1, cAMP response element binding protein 1; TSS, transcription start site.

miR-922 transcripts in liver cancer tissue was determined by *in situ* hybridization using an *In Situ* Hybridization kit (Wuhan Boster Biological Technology Ltd.), according to the manufacturer's protocol. Briefly, liver cancer and adjacent non-cancer tissue sections (thickness, 4 μm) were dewaxed, rehydrated and treated with 3% H_2O_2 for 10 min at room temperature to inactivate endogenous enzymes. The sections were digested with pepsin in 3% citric acid at 37˚C for 30 min and fixed with 4% paraformaldehyde for 5 min at room temperature. After being washed, sections were treated with pre-hybridization solution at 38-42˚C for 2-4 h and hybridized in the presence or absence (negative control) of the probe at 38-42˚C overnight. The sections were washed with 2X saline-sodium citrate and reacted with biotinylated mouse anti-Dig (1:2,000; cat. no. D15041; Bellancom) at 37˚C for 60 min. After being washed, the sections were incubated with streptavidin biotin-peroxidase complex for 60 min at room temperature and reacted with biotinylated peroxidase for 20 min at 37˚C, then visualized with 3,3'-diaminobenzidine (DAB) at room temperature for 10 min and counterstained with hematoxylin. The sections were examined under a light microscope (magnification, x400).

Western blotting. The HepG2 and MHCC97L cells were harvested and lyzed in RIPA lysis buffer (cat. no. P0013B; Beyotime Institute of Biotechnology), followed by centrifugation (9,000 x g; 4˚C; 10 min). After determining the protein concentrations using a BCA kit (Abcam), cell lysates (50 μg/lane) were separated by SDS-PAGE on 12% gels and transferred onto polyvinylidene fluoride membranes (Amersham Pharmacia Biotech; Cytiva). The immunoblot membranes were blocked with 5% fat-free dry milk in TBST (0.1% Tween-20) buffer at 37˚C for 2 h and incubated with primary antibodies overnight at 4˚C (*ARID2*, 1:1,000, cat. no. #82342, Cell Signaling Technology, Inc.; FIGN, 1:1,000, cat. no. ab122238, Abcam). After being washed, the membranes were reacted at room temperature for 1 h with peroxidase-conjugated secondary antibodies (1:10,000; cat. no. ab6721; Abcam). The signals were visualized using enhanced chemiluminescence reagents (GE Healthcare) and quantified by densitometric analysis using ImageJ software (version 1.48; National Institutes of Health).

RNA immunoprecipitation (RIP). A Magna RIP RNA-Binding Protein Immunoprecipitation kit (cat. no. 17-701; Merck Sharp & Dohme) was used for RIP assay according to the manufacturer's instructions. Briefly, miR-922-expressing cells were fixed with 2% formaldehyde for 5 min at room temperature, lysed and sonicated, followed by centrifugation at 12,000 x g

and 4˚C for 1 min. The supernatants were collected and incubated with *ARID2* antibody (1:1,000, cat. no. #82342; Cell Signaling Technology, Inc.) and *FIGN* antibody (1:1,000, cat. no. ab122238, Abcam); overnight at 4˚C. The immunocomplex was precipitated using protein A/G Dynabeads; after being washed, the immunocomplex was digested with proteinase K. Finally, RNA was extracted with TRIzol and the relative levels of miR-922 in the immunocomplex were determined by RT-qPCR, as aforementioned, using specific primers (forward, 5'-ATGGCGTTTTCCCTCTCC-3' and reverse, 5'-TGACGTAGTCCTATTCTCTGC-3').

Cell apoptosis analysis. The number of apoptotic HepG2 and MHCC97L cells was determined by flow cytometry using an Annexin V-FITC Apoptosis Detection kit (Beyotime Institute of Biotechnology), according to the manufacturer's instructions. Briefly, cells were stained with Annexin V-FITC and PI in the dark. After being washed, cells were analyzed by flow cytometry using an Attune Nxt flow cytometer (BD Biosciences) and FlowJo™ software (version 10.7; BD Biosceinces).

Bioinformatics analysis. Genecards (genecards.org/) and Jaspar (jaspar.genereg.net/) were used to predict transcription factor binding to the miR-922 promoter region. In order to determine the potential role of *CREB1* expression in liver cancer, *CREB1* expression levels were searched in liver cancer (n=371) and non-tumor tissue samples (n=50) of The Cancer Genome Atlas (TCGA) database (portal.gdc.cancer.gov/). The association between *CREB1* protein expression levels and the overall survival (OS) of 360 patients with liver cancer was analyzed in The Human Protein Atlas (proteinatlas.org/).

Tumor xenograft. Animal experiments were approved by the Ethical Committee for Animal Research of The Third Xiangya Hospital of Central South University. A total of 25 male Balb/c nude mice (age, 8 weeks; weight, 18-20 g) were obtained from Charles River Laboratories, Inc. and housed in a specific pathogen-free room (temperature, 26˚C; humidity, 50%; 10/14-h light/dark cycle) with free access to autoclaved food and water. Individual mice were injected subcutaneously with $1x10^7$ MHCC97H, MHCC97H-*ARID2*-NC, MHCC97H-*ARID2*-sh, MHCC97H-NC-OE or MHCC97H-*ARID2*-OE cells (n=5/group). After 4 weeks, mice were anesthetized via intraperitoneal injection of 2% pentobarbital sodium (30 mg/kg body weight). The mice were checked for deep anesthesia, including moderate breathing, cardiovascular depression and complete muscle relaxation, and euthanized by cervical dislocation. Tumors were dissected and images were captured. Tumor volume and weight were measured.

ELISA. The levels of serum VEGF and TNF-α in mice were measured by ELISA using VEGF (cat. no. SEA143Mu; Uscnks, Inc.) and TNF-α ELISA kits (cat. no. RAF129R, Biovendor, Inc.). The samples were tested in triplicate and the minimum detectable concentration for VEGF and TNF-α was 10 pg/ml.

Immunohistochemistry. The expression levels of Bax, Bcl-2, PCNA, Cyclin D1, *MMP3*, *MMP9* and *ARID2* in tumor tissue from mice were analyzed by immunohistochemistry. Briefly, tissues were fixed with 4% formaldehyde for 24 h at room temperature and paraffin-embedded at 54˚C for 4 h. The tissue sections (4 μm) were deparaffinized, rehydrated and subjected to antigen retrieval in sodium citrate buffer in a microwave. After being washed, the sections were incubated overnight at 4˚C with primary antibodies against Bax (1:200; cat. no. ab32503; Abcam), Bcl-2 (1:500; cat. no. ab32124; Abcam), PCNA (1:200; cat. no. ab92729; Abcam), Cyclin D1 (1:400; cat. no. ab16663; Abcam), *MMP3* (1:200; cat. no. ab227755; Abcam), *MMP9* (1:200; cat. no. ab119906; Abcam) and *ARID2* (1:400; cat. no. #82342; Cell Signaling Technology, Inc.). The sections were reacted with horseradish peroxidase-conjugated secondary antibodies for 20 min at room temperature and the immunocomplex was viewed using a DAB Detection IHC kit (cat. no. ab64264; Abcam) according to the manufacturer's instructions and counterstained with hematoxylin for 10 sec at room temperature. Images were captured under a light microscope (magnification, x400) and analyzed using Image Pro-Plus (version 6.0; Media Cybernetics, Inc.).

Statistical analysis. Data are expressed as mean ± SD (n=3). All experiments were repeated three times. Statistical analysis was performed using SPSS 22.0 (IBM Corp). Paired student's t-test and one-way ANOVA followed by post hoc Tukey's test were used for comparisons between two or multiple groups, respectively. The survival data were estimated by the Kaplan-Meier method and analyzed by log-rank test. $P<0.05$ was considered to indicate a statistically significant difference.

Results

Elevated miR-922 transcripts in liver cancer tissue. In order to reveal the function of miRNAs in liver cancer progression, differentially expressed miRNAs in liver cancer tissue were screened; miR-922 expression levels were significantly elevated in liver cancer tissue. Expression levels of miR-922 were assessed in 10 pairs of liver cancer and matched adjacent tissue (Table I). miR-922 expression levels in liver cancer tissue were notably higher than in matched adjacent tissue (Fig. 1A, $P<0.05$). Similarly, miR-922 expression increased in HepG2, MHCC97H and MHCC97L cells, relative to non-tumor hepatic THLE-2 cells (Fig. 1B). Hence, upregulated miR-922 expression occurred in liver cancer tissue and may participate in the pathogenesis of liver cancer.

miR-922 enhances malignant behavior of liver cancer cells. In order to determine the effect of altered miR-922 expression on malignant behavior of liver cancer cells, the regulatory role of miR-922 in the proliferation, clonogenicity, wound healing, invasion and apoptosis of HepG2 and MHCC97L cells was assessed *in vitro*. In comparison with control HepG2/MHCC97L and HepG2-NC/MHCC97L-NC, miR-922 over-expression significantly increased proliferation, clonogenicity, would healing and invasion of HepG2 and MHCC97L cells, but decreased the number of apoptotic HepG2/MHCC97L cells (Figs. 1C-G and S1). By contrast, transfection with miR-922 inhibitor exhibited opposite effects on malignant behavior in HepG2 and MHCC97L cells. miR-922 mimics or inhibitor

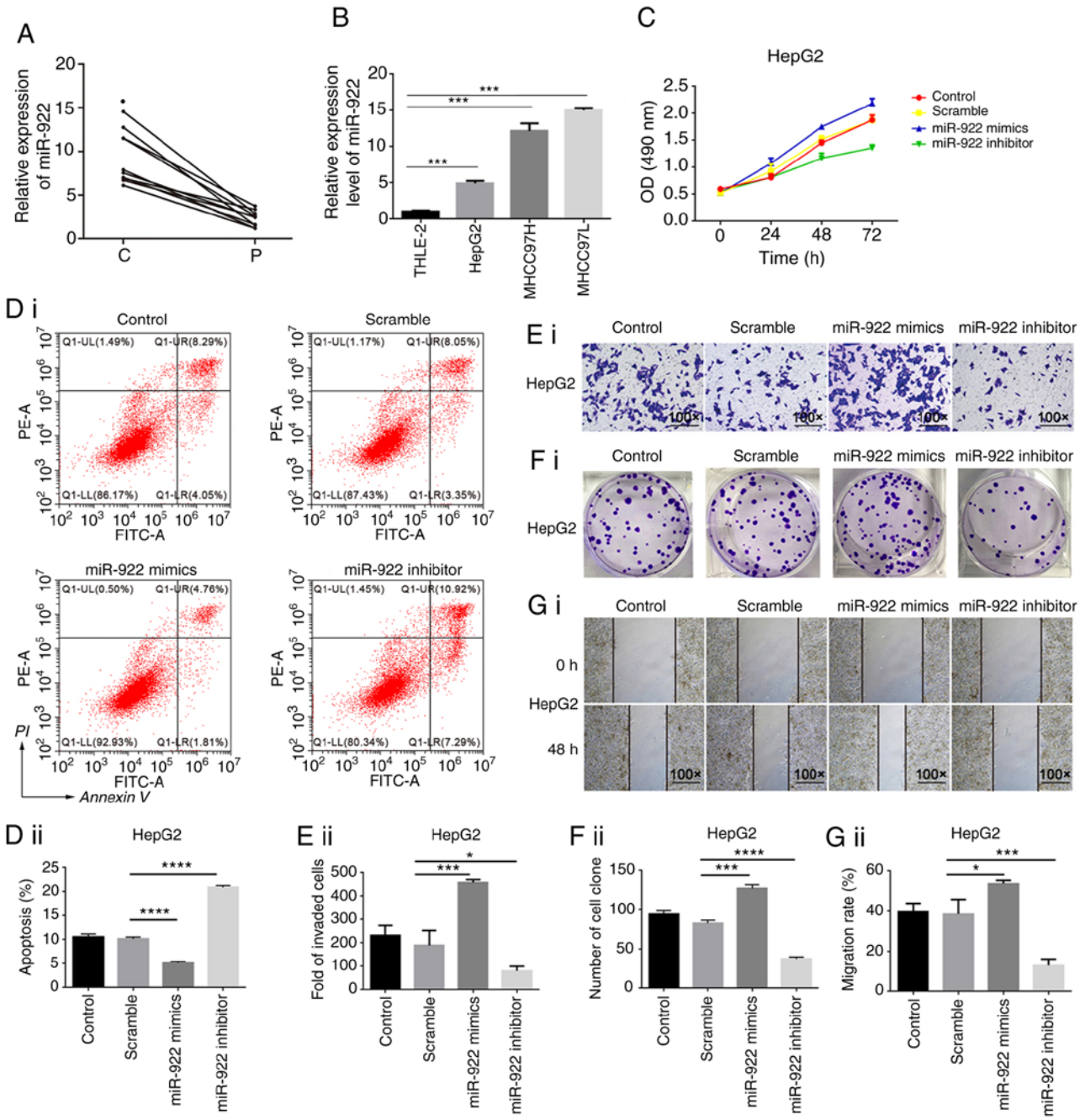

Figure 1. Upregulated miR-922 expression levels promote malignant behavior of liver cancer cells. The relative levels of miR-922 transcripts were determined in 10 pairs of liver cancer and adjacent non-tumor tissue, as well as liver cancer cells and non-tumor hepatocytes by RT-qPCR. (A) RT-qPCR analysis of miR-922 transcripts in liver cancer and adjacent non-tumor tissue (n=10). (B) RT-qPCR analysis of miR-922 transcripts in HepG2, MHCC97H and MHCC97L cells and non-tumor hepatocyte THLE-2 cells. (C) Cell Counting Kit-8 tested the proliferation of liver cancer cells. (Di and Dii) Flow cytometry analyzed the number of apoptotic HepG2 cells in each group. (Ei and Eii) Transwell invasion assays detected HepG2 cell invasion ability. (Fi and Fii) Colony formation assays determined clonogenicity. (Gi and Gii) Wound healing assay assessed the migration ability of HepG2 cells. *P<0.05, ***P<0.001, ****P<0.0001. C, cancer tissue; P, para-carcinoma tissue; miR, microRNA; RT-q, reverse transcription-quantitative; OD, optical density.

was introduced into HepG2 and MHCC97L to overexpress or inhibit the expression of miR-922, respectively. The efficacy of overexpression or inhibition of miR-922 was confirmed by RT-PCR method (Fig. S5).

CREB1 promotes miR-922 transcription. Bioinformatics analysis was performed to predict the potential binding of transcription factors to the promoter region of miR-922 using the GeneCard database; results predicted binding of *CREB1* to the promoter region of miR-922. Accordingly, it was speculated that *CREB1* may enhance expression levels of miR-922 in liver cancer cells. *CREB1* is a key transcription factor that promotes the development and progression of tumors (17). In order to determine whether *CREB1* could regulate miR-922 transcription, the potential binding of *CREB1* to the miR-922 promoter region was assessed by ChIP assay. Anti-*CREB1* antibody precipitated chromatins containing the miR-922 promoter region, indicating that *CREB1* bound to the miR-922 promoter region (Fig. 2A). Similarly, luciferase reporter assay indicated that co-transfection with the plasmid for *CREB1*

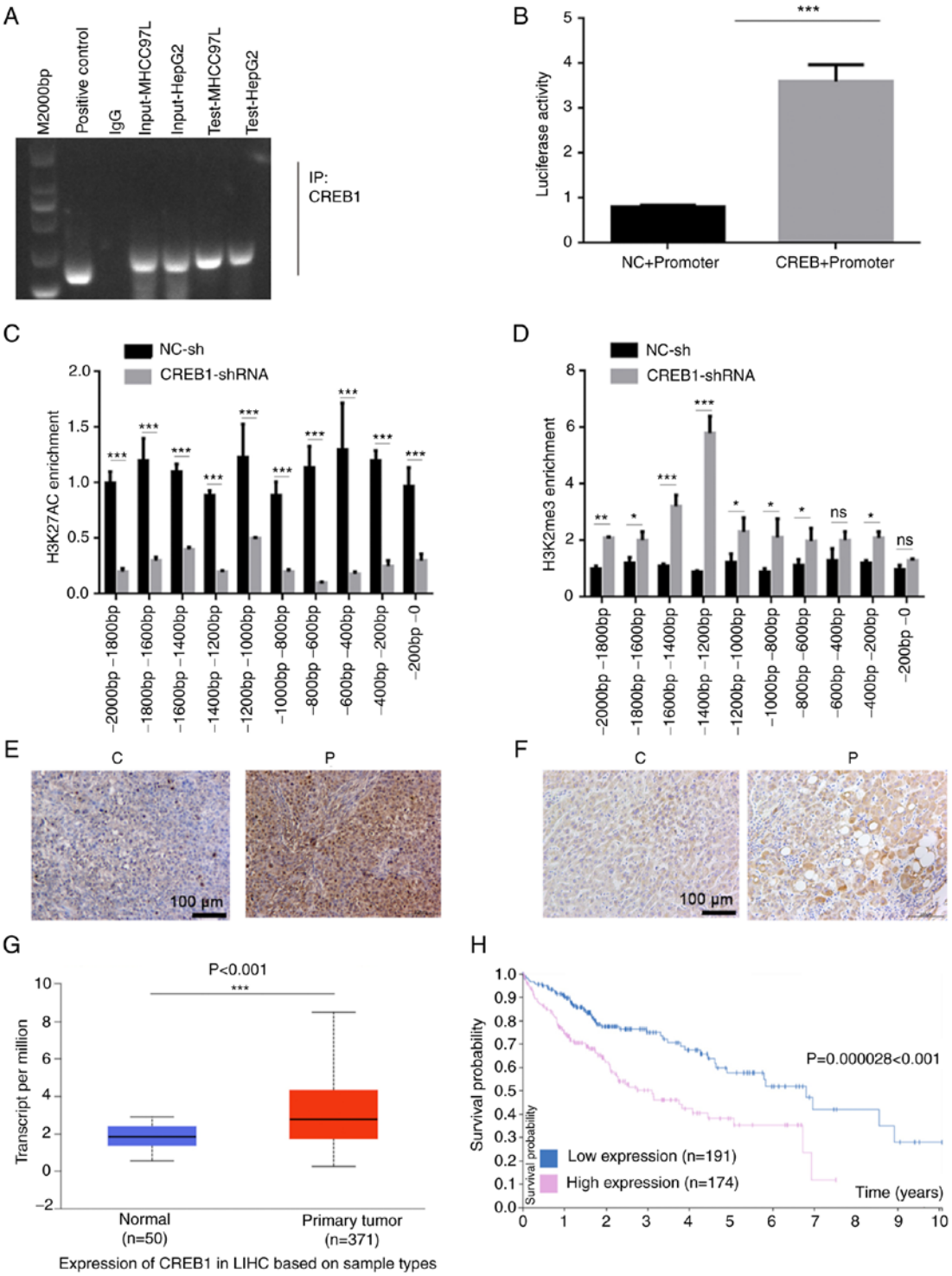

Figure 2. *CREB1* stimulates miR-922 transcription in liver cancer. (A) ChIP-PCR indicated that *CREB1* bound to the miR-922 promoter region. (B) Luciferase assay demonstrated that induction of *CREB1* expression enhanced miR-922 promoter-controlled luciferase expression in 293T cells. ChIP-PCR analyzed enrichment of (C) H3K27AC histone acetyltransferase and (D) H3K27me3 histone methyltransferase on different fragments of the *CREB1* promoter region. (E) *In situ* hybridization demonstrated increased expression levels of miR-922 in liver cancer tissue compared with adjacent non-tumor tissue. (F) Immunohistochemistry showed increased *CREB1* expression levels in liver cancer tissue compared with adjacent non-tumor tissue. (G) miR-922 expression levels are increased in LIHC tissue in The Cancer Genome Atlas database. (H) Higher levels of *CREB1* expression were associated with a shorter overall survival of patients with liver cancer in The Human Protein Atlas database. *P<0.05, **P<0.01, ***P<0.001. *CREB1*, cAMP response element binding protein 1; miR, microRNA; ChIP, chromatin immunoprecipitation; NC, negative control; sh, short hairpin; C, cancer tissue; P, para-carcinoma tissue; ns, not significant; LIHC, liver hepatocellular carcinoma.

expression significantly increased miR-922 promoter activity in 293T cells (Fig. 2B). Furthermore, *CREB1* silencing significantly decreased enrichment of H3K27Ac but elevated that of H3K27me3 in 293T cells (Fig. 2C and D). *In situ* hybridization indicated that the expression levels of miR-922 in liver cancer tissue were higher than in adjacent non-tumor tissue (Fig. 2E). Similarly, miR-922 expression levels in liver cancer tissue were significantly higher than in non-tumor liver

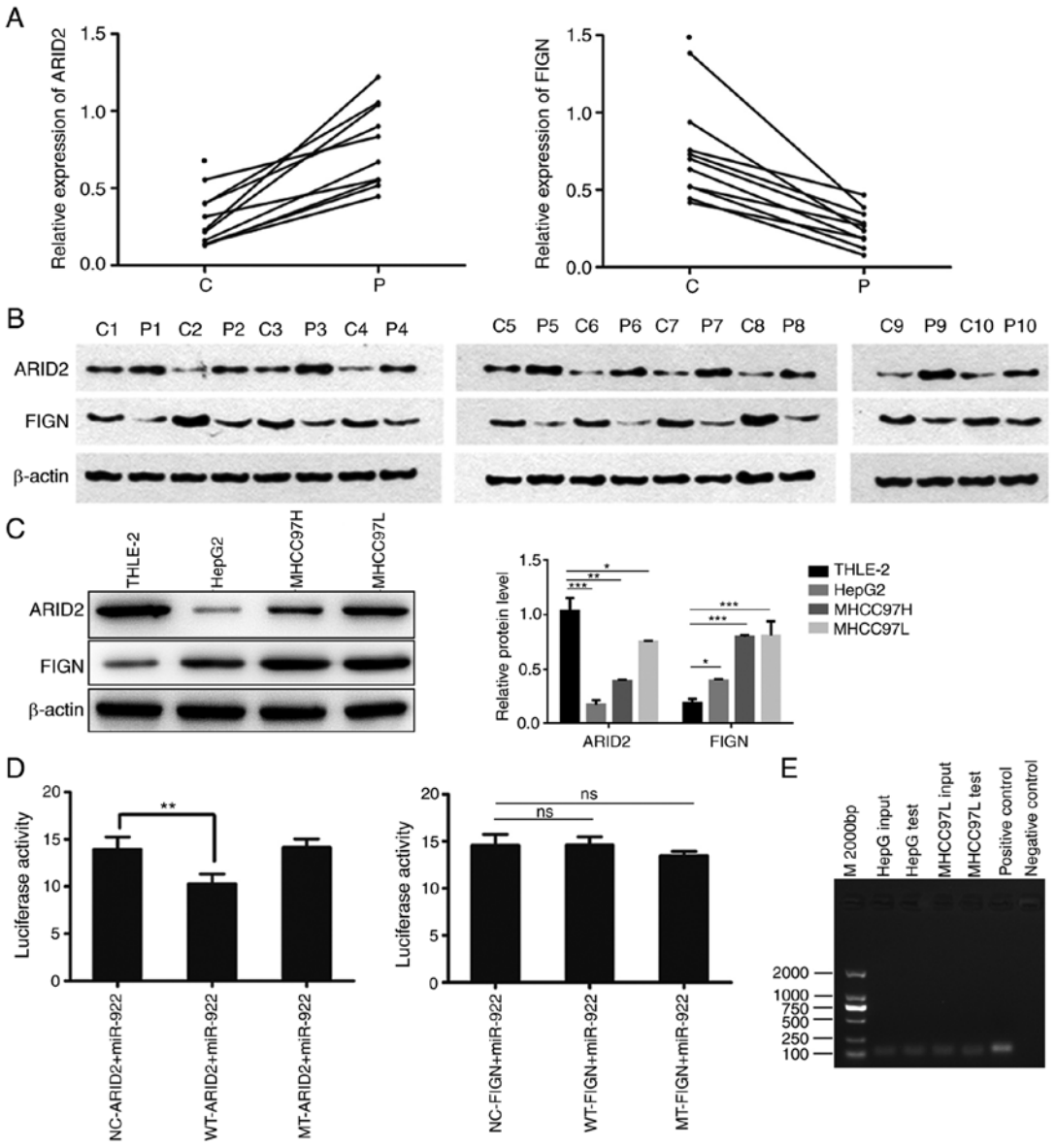

Figure 3. *ARID2* is a potential target of miR-922 in liver cancer. Relative levels of FIGN and *ARID2* expression levels in 10 pairs of liver cancer and adjacent non-tumor tissue were determined by reverse transcription-quantitative PCR and western blot analysis. WT or MT 3'UTR of *FIGN* and *ARID2* were cloned into luciferase reporter vector to generate WT or MT FIGN and *ARID2* luciferase reporter plasmids, respectively. Luciferase reporter gene assay was performed in MHCC97L cells following transfection with miR-922 mimics and plasmid. The presence of miR-922 in miRNA/AGO2 complex was determined by RNA immunoprecipitation using anti-AGO2 antibody. (A) *FIGN* and *ARID2* mRNA transcripts in liver cancer tissue. FIGN and *ARID2* protein expression levels in (B) liver cancer tissue and (C) HepG2, MHCC97H and MHCC97L and non-tumor hepatocyte THLE-2 cells. (D) Luciferase activity. (E) Representative images of agarose gel electrophoresis of PCR products. Data are presented as the mean ± SD (n=3). *P<0.05, **P<0.01, ***P<0.001. C, cancer tissue; P, para-carcinoma tissue; *ARID2*, AT-rich interactive domain 2; miR, microRNA; FIGN, fidgetin, microtubule severing factor; WT, wild-type; MT, mutant; NC, negative control; ns, not significant.

tissue in TCGA database (Fig. 2G). Consistently, immunohistochemistry revealed significantly higher levels of *CREB1* in liver cancer tissue compared with non-tumor tissue (Fig. 2F). Higher levels of *CREB1* expression were significantly associated with a shorter period of OS in patients with liver cancer in The Human Protein Atlas database (P<0.001; Fig. 2H). Together, these data indicated that higher levels of *CREB1* enhanced miR-922 expression levels, promoting progression and poor prognosis of liver cancer.

miR-922 targets ARID2 in liver cancer cells. Potential targeted genes of miR-922 were studied via bioinformatics analysis. Among the predicted targeted genes of miR-922, miR-922 may target *FIGN* and *ARID2* (data not shown). Given that *FIGN* and *ARID2* regulate the development of malignant tumors (12,18), their expression levels were analyzed in 10 pairs of liver cancer tissue by RT-qPCR. *FIGN* mRNA transcripts notably increased, whereas *ARID2* mRNA transcripts were decreased in liver cancer tissue compared with non-tumor tissue (Fig. 3A, P<0.05). A similar pattern of FIGN and *ARID2* protein expression was observed in these tissues by western blotting (Fig. 3B). Moreover, upregulated FIGN and downregulated *ARID2* expression levels were detected in HepG2, MHCC97H and MHCC97L cells compared with in non-tumor hepatic THLE-2 cells (Fig. 3C). In order to clarify the targeting association, WT or MT 3'UTR of *FIGN* and *ARID2* was cloned

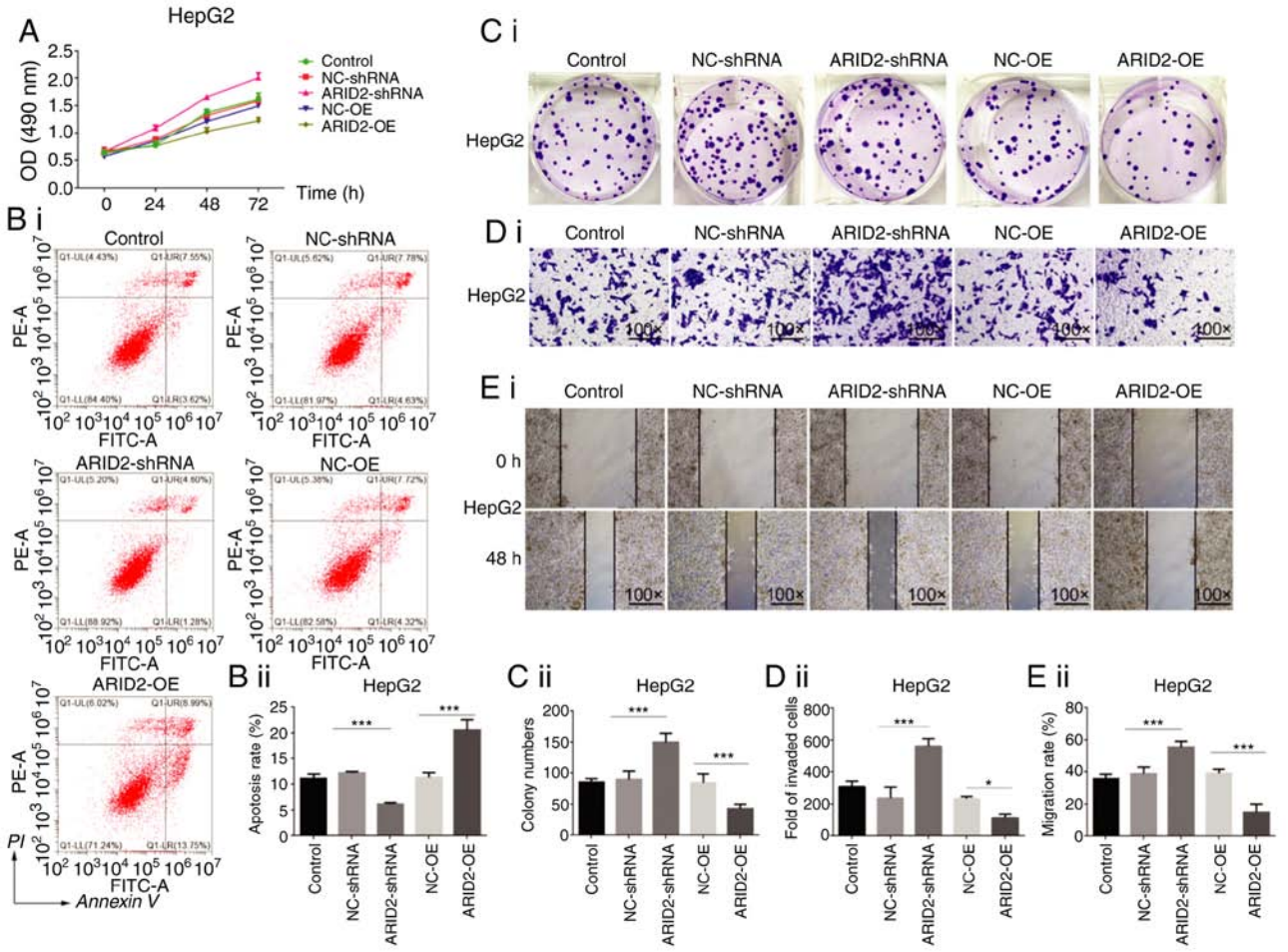

Figure 4. Altered *ARID2* expression changes malignant behavior of liver cancer cells. The proliferation, clonogenicity, apoptosis, wound healing and invasion of HepG2 cells were determined following altered *ARID2* expression. (A) Cell Counting Kit-8 assay determined cell proliferation. (Bi and Bii) Flow cytometry analysis of apoptotic cells. (Ci and Cii) Cell clonogenicity of HepG2 cells. (Di and Dii) Transwell assay analysis of HepG2 cell invasion. (Ei and Eii) Wound healing analysis of HepG2 cell proliferation and migration. Data are presented as the mean ± SD (n=3). *P<0.05, ***P<0.001. *ARID2*, AT-rich interactive domain 2; OD, optical density; NC, negative control; sh, short hairpin; OE, overexpression.

into the luciferase reporter plasmid to generate WT or MT FIGN and *ARID2* luciferase reporter plasmid, respectively. Following co-transfection, dual luciferase reporter assay indicated that co-transfection with miR-922 mimics significantly decreased *ARID2*-regulated, but not MT-*ARID2*-regulated, luciferase activity in MHCC97L cells (P<0.01); WT-FIGN or MT-FIGN-regulated luciferase activity was not affected in MHCC97L cells (Fig. 3D). These data suggest that miR-922 may target *ARID2* to decrease its expression in liver cancer. RIP assays using anti-AGO2 detected miR-922 in HepG2 and MHCC97L cells (Fig. 3E), indicating that miR-922 existed in the miR-922/AGO2 complex. These data suggest that miR-922 may target *ARID2* and decrease its expression to modulate malignant behavior of liver cancer cells.

Altered ARID2 expression modulates malignant behavior of liver cancer cells. *ARID2* is a tumor suppressor and serves as a genetic modulator during the progression of several types of cancers, including liver cancer (12). The regulatory role of *ARID2* in the malignant behavior of HepG2 and MHCC97L cells was investigated by CCK-8, colony formation, wound healing, apoptosis and Transwell invasion assays *in vitro*. The *ARID2* cDNA sequence was cloned into pcDNA3.1 vector for gene over-expression and three *ARID2* specific shRNA were cloned into pGUP6 vector for stable gene-silence. The protein level of *ARID2* in HEK293 was determined after transduction with either *ARID2*-pcDNA3.1 or sh-*ARID2* plasmid. As shown in figure, the *ARID2* expression was significantly increased in *ARID2*-pcDNA3.1 group and was dramatically reduced in sh-*ARID2* group compared to the control group. Among three *ARID2* specific shRNA, sh-*ARID2*-2 achieved most robust knockdown efficiency, which then was used in following experiment (Fig. S6). In comparison with the control NC-OE and NC-sh cells, *ARID2* over-expression significantly decreased proliferation, clonogenicity, wound healing and invasion, but increased the number of apoptotic HepG2 and MHCC97L cells (Figs. 4 and S2). By contrast, *ARID2* silencing exhibited opposite effects on the malignant behavior of HepG2 and MHCC97L cells.

Similarly, *ARID2* over-expression in MHCC97L cells significantly decreased tumor volume and weight *in vivo*, whereas *ARID2* silencing in MHCC97L cells did not significantly alter tumor volume and weight in mice (Fig. 5A-C). Furthermore, *ARID2* over-expression significantly decreased miR-922 expression levels, whereas *ARID2* silencing increased its expression in xenografts (Fig. 5D), suggesting that *ARID2* may regulate

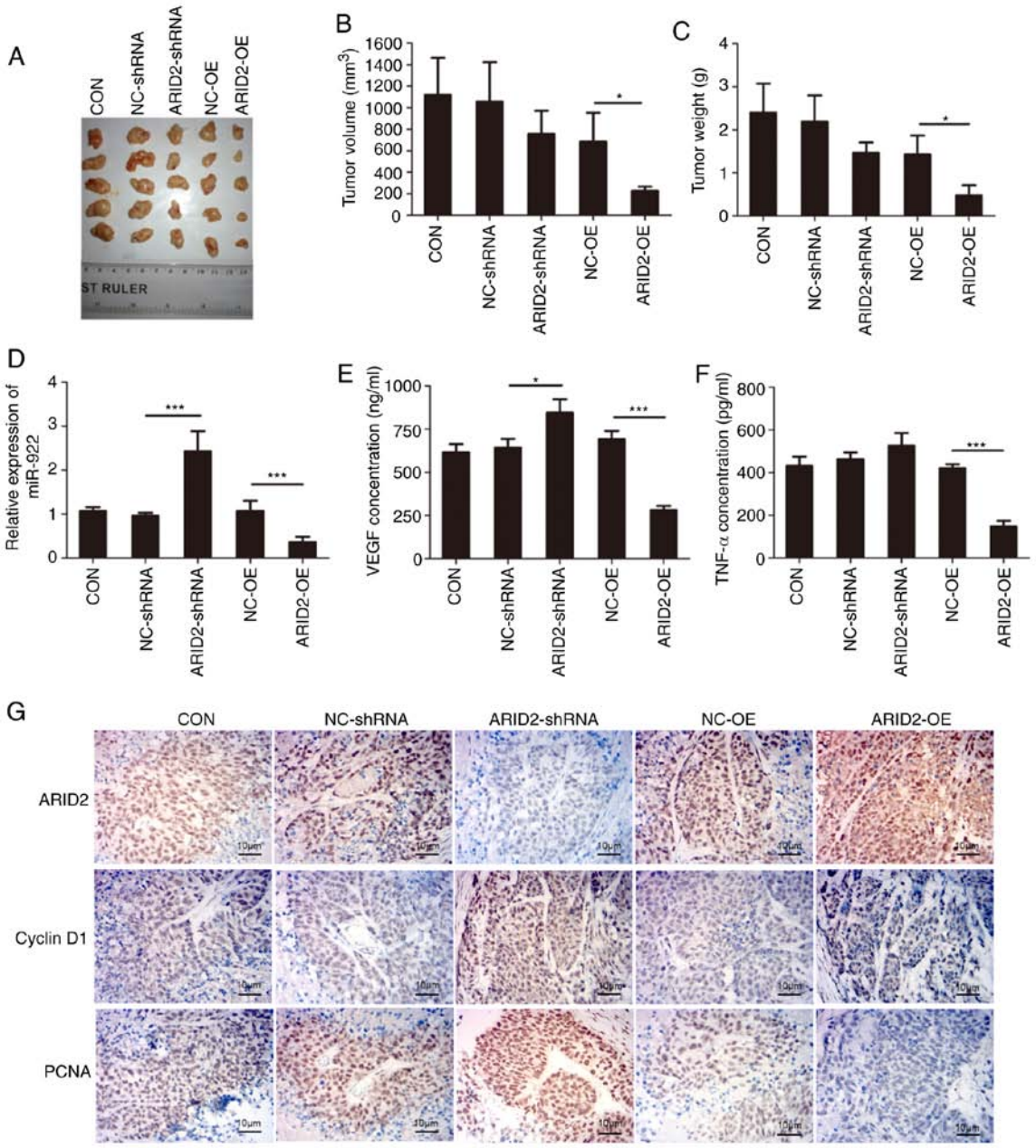

Figure 5. Altered *ARID2* expression modulates the growth of xenograft liver cancer tumor in mice. Male Balb/c nude mice were injected subcutaneously with $1x10^7$ cells; 28 days later, tumor tissue was dissected and volume and weight were measured. The relative levels of miR-922 expression in tumor tissue were determined by reverse transcription-quantitative PCR and the levels of serum VEGF and TNF-α in mice were measured by ELISA. *ARID2*, Bcl-2, Bax, PCNA, Cyclin D1, *MMP3* and *MMP9* expression levels in tumor tissue were characterized by immunohistochemistry. (A) Tumor-bearing mice. Tumor (B) volume and (C) weight. (D) Relative levels of miR-922 transcripts in tumor tissue. ELISA analysis of serum (E) VEGF and (F) TNF-α levels in mice. (G) Immunohistochemistry analysis of *ARID2*, Bcl-2, Bax, PCNA, cyclin D1, *MMP3* and *MMP9* expression levels in tumor tissue. Data are presented as the mean ± SD (n=3). *P<0.05, ***P<0.001. *ARID2*, *ARID2*, AT-rich interactive domain 2; PCNA, proliferating cell nuclear antigen; CON, control; NC, negative control; sh, short hairpin; OE, over-expression.

miR-922 expression. In addition, *ARID2* over-expression significantly decreased serum levels of VEGF and TNF-α, whereas *ARID2* silencing elevated the serum levels of VEGF and TNF-α in tumor-bearing mice (Fig. 5E and F). Immunohistochemistry revealed that *ARID2* over-expression increased *ARID2* and Bax expression levels, but decreased those of cyclin D1, PCNA, BcL-2, *MMP3* and *MMP9* in liver cancer xenografts (Figs. 5G and S3). By contrast, *ARID2* silencing exhibited opposite effects on expression levels in liver cancer xenografts (Figs. 5G and S3). Collectively, these data demonstrated that *ARID2* mitigated malignant behavior of liver cancer cells.

Altered ARID2 expression modulates miR-922 inhibitor-decreased malignant behavior of liver cancer cells. Finally, it was determined whether altered *ARID2* expression modulates miR-922 inhibitor-decreased malignant behavior of liver cancer cells. *ARID2* over-expression enhanced miR-922 inhibitor-decreased proliferation, clonogenicity, invasion and wound healing of HepG2 cells and increased the number of apoptotic HepG2 cells (Fig. 6). By contrast, *ARID2* silencing mitigated miR-922 inhibitor-decreased malignant behavior of HepG2 cells (Fig. 6). Similar effects of altered *ARID2* expression on miR-922 inhibitor-decreased malignant behavior were

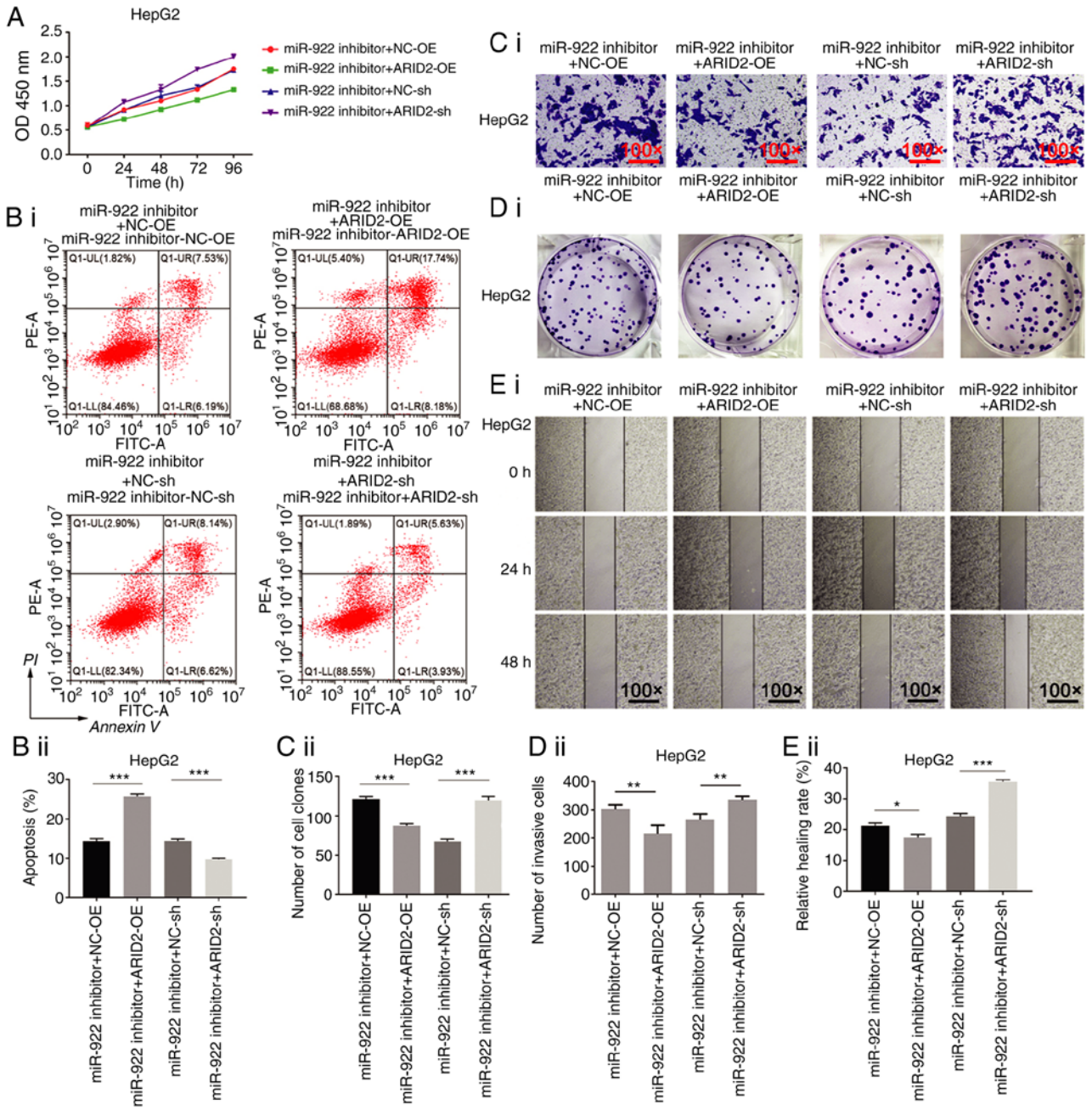

Figure 6. Altered *ARID2* expression modulates miR-922 inhibitor-decreased malignant behavior of HepG2 cells. HepG2 cells were stably transfected with miR-922 inhibitor and transfected with plasmid for *ARID2* expression or *ARID2*-specific shRNA for *ARID2* silencing. Control cells were transfected with vehicle. (A) Cell Counting Kit-8 determined cell proliferation. (Bi and Bii) Number of apoptotic HepG2 cells was analyzed by flow cytometry. (Ci and Cii) Clonogenicity of each group of HepG2 cells was analyzed by colony formation assay. (Di and Dii) Wound healing analysis of each group of HepG2 cells. (Ei and Eii) Transwell assay analysis determined the invasion of each group of HepG2 cells. Data are presented as the mean ± SD (n=3). *P<0.05, **P<0.01, ***P<0.001. *ARID2*, AT-rich interactive domain 2; miR, microRNA; sh, short hairpin; OD, optical density; NC, negative control; OE, over-expression.

observed in MHCC97L cells (Fig. S4). These data indicated that miR-922-regulated *ARID2* expression was key for control of malignant behavior of liver cancer cells.

Discussion

A previous study verified that miRNAs regulate hepatocarcinogenesis (19). miR-221/222, miR-34a and miR-224 serve as oncogenes to promote tumor cell growth (20,21), while miR-122 and miR-375 suppress tumor progression by inhibiting liver cancer cell invasion and metastasis (17,22). Previous studies have shown that miR-922 expression is upregulated in liver cancer (23) and miR-922 promotes the proliferation of liver cancer cells by targeting *CYLD* to enhance c-Myc and cyclin D1 expression levels and inhibit Rb phosphorylation (7). However, the molecular mechanisms underlying the oncogenic role of miR-922 are still unclear.

The present study found significantly elevated levels of miR-922 transcripts in liver cancer tissue compared with non-tumor adjacent tissue, consistent with a previous study (7). In addition, miR-922 expression levels were upregulated in liver cancer cell lines compared with non-tumor hepatocytes.

Induction of miR-922 over-expression enhanced malignant behavior, rapid proliferation, strong clonogenicity, lower numbers of apoptotic cells, potent would healing and invasion ability in liver cancer cells. All these data indicate that miR-922 may serve as an oncogenic factor to promote malignant behavior of liver cancer cells.

Multiple factors regulate the transcription of miRNAs, including genetic abnormality, epigenetic regulation and transcription factors (24). *CREB1*, a leucine zipper-type transcription factor, regulates numerous types of malignancy (25). A previous study demonstrated that *CREB1* transcriptionally regulates a number of miRNAs (17). The present data indicated that *CREB1* bound to the miR-922 promoter region and stimulated its transcription. Inhibition of *CREB1* decreased H3K27 acetylation upstream of the miR-922 promoter region but enhanced repressive H3K27 trimethylation. These results suggested that *CREB1* may serve as a transcription factor to induce miR-922 expression in liver cancer cells. Future studies should investigate the potential role of other transcription factors in regulating miR-922 expression in liver cancer. In addition, *CREB1* was upregulated in liver cancer tissue and positively associated with miR-922 expression levels. Increased *CREB1* expression levels were associated inversely with OS of patients with liver cancer. Hence, high levels of *CREB1* and miR-922 may be valuable for the prognosis of liver cancer.

In order to identify the targeted genes of miR-922 and the underlying mechanisms, potential targeted genes of miR-922 were predicted; miR-922 targeted *ARID2*. *ARID2* is a tumor suppressor and subunit of SWitch/sucrose non-fermentable complex B (26). Given that *ARID2* mutations are associated with the development of HCC (27-29), targeting *ARID2* by miR-922 may promote malignant behavior of HCC. *ARID2* over-expression eliminated malignant behavior of liver cancer cells whereas *ARID2* silencing had opposite effects, consistent with a previous report (30). In addition, *ARID2* over-expression significantly mitigated or abrogated miR-922-promoted malignant behavior of liver cancer cells. *ARID2* over-expression also enhanced Bax expression levels, but decreased those of Bcl-2, PCNA, cyclin D1, *MMP3* and *MMP9* in liver cancer tumors, which explained why *ARID2* over-expression inhibited growth of implanted liver cancer xenografts in mice. Previous studies have shown that *ARID2* is targeted by miR-376c-3p, miR-208-3p and miR-155 in HCC (30-32). Accordingly, the present findings extended previous observations and indicate that the miR-922/*ARID2* axis is key for regulating malignant behavior of liver cancer cells (33) and that miR-922 may collaborate with other miRNAs to attenuate *ARID2* expression levels, which promotes development and progression of liver cancer. Further investigation is required to determine whether miR-922 directly interacts with *ARID2* mRNA in liver cancer cells.

Together, the present data indicated significantly upregulated miR-922 expression levels in liver cancer tissue and cells; its elevated expression was associated with *CREB1* expression levels in liver cancer tissue. Both *in vitro* and *in vivo* experiments demonstrated that miR-922 enhanced malignancy of liver cancer by promoting tumor growth and cell proliferation, wound healing and invasion. Mechanistically, these findings may provide novel insights into the *CREB1*/miR-922/*ARID2* interaction network in liver cancer progression. Therefore, miR-922 may be a valuable diagnostic and prognostic biomarker for liver cancer; targeting the *CREB1*/miR-922/*ARID2* axis may represent a new therapeutic strategy for intervention of liver cancer. The present study had limitations, including limited sample size of patients with HCC with chronic hepatitis B, but not with other risk factors, such as hepatitis B core and alcoholic liver disease. Therefore, further studies with a larger population of patients with liver cancer with diverse risk factors are warranted to validate the role of the *CREB1*/*ARID2*/miR-922 axis in the progression of liver cancer.

Acknowledgements

Not applicable.

Funding

The present study was supported by grants from Hunan Provincial Natural Science Foundation (grant no. 2019JJ40495) and Guangxi Provincial Natural Science Foundation (grant no. 2018GXNSFDA281003).

Availability of data and materials

The datasets used and analyzed during the current study are available from the corresponding author upon reasonable request.

Authors' contributions

XL and ZL designed the study. XL, HZ, PZ, HYZ, LC and JG performed the experiments. XL and YY collected the data. HZ, PZ, YY, LC and JG analyzed the data. XL, HZ, PZ, YY, HYZ, LC and JG interpreted the data. XL and ZL drafted the manuscript. HZ and PZ revised the manuscript. All authors read and approved the final manuscript. All authors confirm the authenticity of all the raw data.

Ethics approval and consent to participate

The present study was approved by the Ethics Committee of the Third Xiangya Hospital of Central South University (approval no. 2020-S362). All participants provided written informed consent.

Patient consent for publication

Not applicable.

Competing interests

The authors declare that they have no competing interests.

References

1. Singh AK, Kumar R and Pandey AK: Hepatocellular carcinoma: Causes, mechanism of progression and biomarkers. Curr Chem Genom Transl Med 12: 9-26, 2018.
2. Zhu X, Tang Z and Sun HC: Targeting angiogenesis for liver cancer: Past, present, and future. Genes Dis 7: 328-335, 2020.
3. Sagnelli E, Potenza N, Onorato L, Sagnelli C, Coppola N and Russo A: Micro-RNAs in hepatitis B virus-related chronic liver diseases and hepatocellular carcinoma. World J Hepatol 10: 558-570, 2018.

4. Sengupta S and Parikh ND: Biomarker development for hepatocellular carcinoma early detection: Current and future perspectives. Hepat Oncol 4: 111-122, 2017.
5. Rupaimoole R, Calin GA, Lopez-Berestein G and Sood AK: miRNA deregulation in cancer cells and the tumor microenvironment. Cancer Discov 6: 235-246, 2016.
6. Shayimu P, Wang JB, Liu L, Tuerdi R, Yu CG and Yusufu A: miR-922 regulates apoptosis, migration, and invasion by targeting SOCS1 in gastric cancer. Kaohsiung J Med Sci 36: 178-185, 2020.
7. Liu J, Su Z, Zeng Y, Zhang H, Yang S and Liu G: miR-922 regulates CYLD expression and promotes the cell proliferation of human hepatocellular carcinoma. Oncol Rep 37: 1445-1450, 2017.
8. Sevinc ED, Cecener G, Ak S, Tunca B, Egeli U, Gokgoz S, Tolunay S and Tasdelen I: Expression and clinical significance of miRNAs that may be associated with the FHIT gene in breast cancer. Gene 590: 278-284, 2016.
9. Abramovitch R, Tavor E, Jacob-Hirsch J, Zeira E, Amariglio N, Pappo O, Rechavi G, Galun E and Honigman A: A pivotal role of cyclic AMP-responsive element binding protein in tumor progression. Cancer Res 64: 1338-1346, 2004.
10. Kovach SJ, Price JA, Shaw CM, Theodorakis NG and McKillop IH: Role of cyclic-AMP responsive element binding (CREB) proteins in cell proliferation in a rat model of hepatocellular carcinoma. J Cell Physiol 206: 411-419, 2006.
11. Li Y, Fu Y, Hu X, Sun L, Tang D, Li N, Peng F and Fan XG: The HBx-CTTN interaction promotes cell proliferation and migration of hepatocellular carcinoma via CREB1. Cell Death Dis 10: 405, 2019.
12. Oba A, Shimada S, Akiyama Y, Nishikawaji T, Mogushi K, Ito H, Matsumura S, Aihara A, Mitsunori Y, Ban D, *et al*: ARID2 modulates DNA damage response in human hepatocellular carcinoma cells. J Hepatol 66: 942-951, 2017.
13. Marrero JA, Kulik LM, Sirlin CB, Zhu AX, Finn RS, Abecassis MM, Roberts LR and Heimbach JK: Diagnosis, staging, and management of hepatocellular carcinoma: 2018 practice guidance by the American association for the study of liver diseases. Hepatology 68: 723-750, 2018.
14. Tellapuri S, Sutphin PD, Beg MS, Singal AG and Kalva SP: Staging systems of hepatocellular carcinoma: A review. Indian J Gastroenterol 37: 481-491, 2018.
15. Livak KJ and Schmittgen TD: Analysis of relative gene expression data using real-time quantitative PCR and the 2(-Delta Delta C(T)) method. Methods 25: 402-408, 2001.
16. Zhu P, Wang Y, Wu J, Huang G, Liu B, Ye B, Du Y, Gao G, Tian Y, He L and Fan Z: LncBRM initiates YAP1 signalling activation to drive self-renewal of liver cancer stem cells. Nat Commun 7: 13608, 2016.
17. Wang YW, Chen X, Ma R and Gao P: Understanding the CREB1-miRNA feedback loop in human malignancies. Tumour Biol 37: 8487-8502, 2016.
18. Rad R, Rad L, Wang W, Strong A, Ponstingl H, Bronner IF, Mayho M, Steiger K, Weber J, Hieber M, *et al*: A conditional piggyBac transposition system for genetic screening in mice identifies oncogenic networks in pancreatic cancer. Nat Genet 47: 47-56, 2015.
19. Xu J, Li J, Zheng TH, Bai L and Liu ZJ: MicroRNAs in the occurrence and development of primary hepatocellular carcinoma. Adv Clin Exp Med 25: 971-975, 2016.
20. Pineau P, Volinia S, McJunkin K, Marchio A, Battiston C, Terris B, Mazzaferro V, Lowe SW, Croce CM and Dejean A: miR-221 overexpression contributes to liver tumorigenesis. Proc Natl Acad Sci USA 107: 264-269, 2010.
21. Varnholt H: The role of microRNAs in primary liver cancer. Ann Hepatol 7: 104-113, 2008.
22. He XX, Chang Y, Meng FY, Wang MY, Xie QH, Tang F, Li PY, Song YH and Lin JS: MicroRNA-375 targets AEG-1 in hepatocellular carcinoma and suppresses liver cancer cell growth in vitro and in vivo. Oncogene 31: 3357-3369, 2012.
23. Liu Y, Chen SH, Jin X and Li YM: Analysis of differentially expressed genes and microRNAs in alcoholic liver disease. Int J Mol Med 31: 547-554, 2013.
24. Lee YS and Dutta A: MicroRNAs in cancer. Annu Rev Pathol 4: 199-227, 2009.
25. Hu PC, Li K, Tian YH, Pan WT, Wang Y, Xu XL, He YQ, Gao Y, Wei L and Zhang JW: CREB1/Lin28/miR-638/VASP interactive network drives the development of breast cancer. Int J Biol Sci 15: 2733-2749, 2019.
26. Hodges C, Kirkland JG and Crabtree GR: The many roles of BAF (mSWI/SNF) and PBAF complexes in cancer. Cold Spring Harb Perspect Med 6: a026930, 2016.
27. Linhares AC, Stupka JA, Ciapponi A, Bardach AE, Glujovsky D, Aruj PK, Mazzoni A, Rodriguez JA, Rearte A, Lanzieri TM, *et al*: Burden and typing of rotavirus group A in Latin America and the Caribbean: Systematic review and meta-analysis. Rev Med Virol 21: 89-109, 2011.
28. Zhao H, Wang J, Han Y, Huang Z, Ying J, Bi X, Zhao J, Fang Y, Zhou H, Zhou J, *et al*: ARID2: A new tumor suppressor gene in hepatocellular carcinoma. Oncotarget 2: 886-891, 2011.
29. You J, Yang H, Lai Y, Simon L, Au J and Burkart AL: AT-rich interactive domain 2, p110α, p53, and β-catenin protein expression in hepatocellular carcinoma and clinicopathologic implications. Hum Pathol 46: 583-592, 2015.
30. Zhang L, Wang W, Li X, He S, Yao J, Wang X, Zhang D and Sun X: MicroRNA-155 promotes tumor growth of human hepatocellular carcinoma by targeting ARID2. Int J Oncol 48: 2425-2434, 2016.
31. Wang Y, Chang W, Chang W, Chang X, Zhai S, Pan G and Dang S: MicroRNA-376c-3p facilitates human hepatocellular carcinoma progression via repressing AT-rich interaction domain 2. J Cancer 9: 4187-4196, 2018.
32. Yu P, Wu D, You Y, Sun J, Lu L, Tan J and Bie P: miR-208-3p promotes hepatocellular carcinoma cell proliferation and invasion through regulating ARID2 expression. Exp Cell Res 336: 232-241, 2015.
33. Liu Q, Yang P, Tu K, Zhang H, Zheng X, Yao Y and Liu Q: TPX2 knockdown suppressed hepatocellular carcinoma cell invasion via inactivating AKT signaling and inhibiting MMP2 and MMP9 expression. Chin J Cancer Res 26: 410-417, 2014.